

## NEAR-INFRARED WATER LINES IN V838 MONOCEROTIS

D. P. K. BANERJEE,<sup>1</sup> R. J. BARBER,<sup>2</sup> N. M. ASHOK,<sup>1</sup> AND J. TENNYSON<sup>2</sup>

*Received 2005 April 19; accepted 2005 June 1; published 2005 June 28*

### ABSTRACT

V838 Monocerotis had an intriguing, nova-like outburst in 2002 January that has subsequently led to several studies of the object. It is now recognized that the outburst of V838 Mon and its evolution are different from those of a classical nova or other classes of well-known eruptive variables. V838 Mon, along with two other objects that have analogous properties, appears to make up a new class of eruptive variables. There are limited infrared studies of V838 Mon. Here we present near-infrared *H*-band (1.5–1.75  $\mu\text{m}$ ) spectra of V838 Mon from late 2002 to the end of 2004. The principal new result from our work is the detection of several rotation-vibration lines of water in the *H*-band spectra. The observed water lines have been modeled to first establish that they are indeed due to water. Subsequently the temperature and column densities of the absorbing material, from where the water absorption features originate, are derived. From our analysis, we find that the water features arise from a cool,  $\sim 750$ – $900$  K, region around V838 Mon that appears to be gradually cooling with time.

*Subject headings:* infrared: stars — novae, cataclysmic variables — stars: individual (V838 Monocerotis) — techniques: spectroscopic

### 1. INTRODUCTION

Water vapor is the most important gas-phase molecule in astrophysical environments after  $\text{H}_2$  and CO. It is an abundant molecule in the atmospheres of cool, oxygen-rich ( $\text{O}/\text{C} > 1$ ) stars, and it constitutes the major opacity source in the infrared in such stars. The detection of water vapor through clearly identified spectral lines, while not a common event, has been made in a variety of sources. Some of the previous detections are in the photospheres of K and M giants and supergiants (e.g.,  $\alpha$  Ori and  $\alpha$  Sco, Jennings & Sada 1998;  $\alpha$  Boo, Ryde et al. 2002;  $\alpha$  Tau and other stars, Tsuji 2001), in sunspots (Wallace et al. 1995; Polyansky et al. 1997), in young stellar objects (Carr et al. 2004), and in comets (Crovisier et al. 1997; Dello Russo et al. 2005). Detection in other sources such as Herbig-Haro objects, star-forming regions, planetary atmospheres, and outflows from evolved stars such as VY CMa are described by Neufeld et al. (1999 and references therein). From a survey of the literature, it appears that the detection of water lines in novae or nova-like variables is either rare or has not been made earlier. Most of the water detections described above are in the infrared region at wavelengths beyond the *K* band (i.e., beyond 2.4  $\mu\text{m}$ ). Several of them were made by the *Infrared Space Observatory* from spectra obtained in the 2.48–40  $\mu\text{m}$  region. In the *JHK* (1.0–2.4  $\mu\text{m}$ ) region or its vicinity, there are limited reports of water line detections. In this context, we note the detection by Spinrad & Newburn (1965) of a water band at  $\sim 9400$  Å in the spectra of cool M-type stars, and also the detection of water bands in the Mira variable R Leo by Hinkle & Barnes (1979) from high-resolution spectra.

V838 Mon was reported in eruption on 2002 January 6 by Brown (2002). This initial outburst had a peak magnitude of  $V_{\text{max}} = 10$ . Subsequent observations showed two more outbursts in the object (reaching a  $V_{\text{max}}$  of 6.7 and 7, respectively) within the next 2 months. V838 Mon also showed fast cooling to a cool, late M spectral type. The multi-peaked light curve

and the decrease of the effective temperature with time suggested that the object was different from a classical nova. The early photometric and spectroscopic observations are described by Munari et al. (2002), Kimeswenger et al. (2002), Crause et al. (2003), and Wisniewski et al. (2003b). An expanding light echo was also seen around the star (Henden et al. 2002; Bond et al. 2003). Estimates based on the expanding light echo suggest that the object is at a large distance, in the 8–10 kpc range (Tylenda 2004; Crause et al. 2005; van Loon et al. 2004). There is some debate about whether the scattering medium causing the light echo is an interstellar sheet of dust in the line of sight or matter lost in an earlier episode from the progenitor of V838 Mon—which would thereby imply it to be an evolved red giant or asymptotic giant branch star (van Loon et al. 2004; Tylenda et al. 2004). Several suggestions have been made, that V838 Mon has similar properties to V4332 Sgr and M31-RV (two other objects that have erupted in the last 10–15 yr), and that these objects taken together could form a new class of eruptive variables. Our recent results on V4332 Sgr certainly show it to be an unusual object (Banerjee & Ashok 2004; Banerjee et al. 2004). Since the outburst properties of V838 Mon are different from those of known eruptive variables, new mechanisms have been proposed for the outbursts in such objects. Soker & Tylenda (2003) propose a merger between main-sequence stars, while Retter & Marom (2003) suggest a planetary capture for the eruption. In the case of V4332 Sgr specifically, observations suggest that the second mechanism could be plausible (Banerjee et al. 2004). V838 Mon has been the subject of several other studies, viz., polarization studies (Desidera et al. 2004; Wisniewski et al. 2003a), elemental abundance determinations (Kipper et al. 2004; Kaminsky & Pavlenko 2005), interferometric measurements to determine the size of the object (Lane et al. 2005), and investigations of the progenitor of V838 Mon (Munari et al. 2005; Tylenda et al. 2004). However, many aspects of V838 Mon still remain unclear, including a definitive cause for its eruption.

There are two studies of V838 Mon in the infrared that are specially relevant to the present work. Evans et al. (2003), based on an IR spectrum obtained in 2002 October in the 0.8–2.5  $\mu\text{m}$  region, showed that the spectrum of V838 Mon has similarities to a cool L-type dwarf. Lynch et al. (2004), using

<sup>1</sup> Physical Research Laboratory, Navrangpura, Ahmedabad 380009, India; orion@prl.ernet.in, ashok@prl.ernet.in.

<sup>2</sup> Department of Physics and Astronomy, University College London, Gower Street, London WC1E 6BT, UK; bob@theory.phys.ucl.ac.uk, j.tennyson@ucl.ac.uk.

TABLE 1  
LOG OF OBSERVATIONS FOR V838 MONOCEROTIS

DATE (UT)	V838 MON		
	Int. Time (s)	Air Mass	HR 2714 <sup>a</sup> AIR MASS
2002 Nov 20.9056 .....	20	1.114	1.148
2003 Jan 25.8000 .....	45	1.203	1.161
2003 Dec 14.8771 .....	40	1.144	1.109
2004 Apr 15.6542 .....	30	1.655	1.567
2004 Dec 25.8250 .....	60	1.150	1.080

<sup>a</sup> Comparison star.

multiepoch IR spectra between 2002 January and 2003 March, computed a detailed model of V838 Mon and its circumstellar environment. Their model indicates a cool central star with a photospheric temperature of  $\sim 2100$  K surrounded by a large, spherical envelope of molecular matter at  $\sim 750$ – $800$  K. In both these studies, the authors point out the presence of water in V838 Mon (see Figs. 1 and 2 of Evans et al. 2003 and Figs. 6 and 7 of Lynch et al. 2004). In these figures, the presence of water is indicated through the wide and deep absorption troughs seen between the spectral bands, for example, at  $1.4 \mu\text{m}$  between the *J* and *H* bands and at  $1.9 \mu\text{m}$  between the *H* and *K* bands. Such interband water features are well known and commonly observed in cool M stars (see, e.g., the IR catalog of stellar spectra by Lançon & Rocca-Volmerange 1992) and also in brown dwarfs (e.g., the spectral catalog by Geballe et al. 2002). In addition, Figure 12 of Lynch et al. (2004) shows water lines in the *K* band in both their model and observed data. However, the studies by Evans et al. (2003) and Lynch et al. (2004) do not identify and label specific water lines as we do here. Furthermore, our spectra extend to late 2004, beyond the observations reported in the above studies.

## 2. OBSERVATIONS

Since its outburst in early 2002, near-IR *JHK* spectra of V838 Mon have been taken, until the present day, at approximately bimonthly intervals from the 1.2 m telescope at Mount Abu Observatory. Observations from mid-June to early October are not possible, because of the rainy season. Spectra early after the outburst (until 2002 May) are presented in Banerjee & Ashok (2002). The *H*-band spectra presented here cover the period from the end of 2002 to the end of 2004 and are taken at fairly equally spaced epochs—they are thus suitable to study the evolution of the object. The present spectra, like those of our earlier study, were obtained at a resolution of  $\sim 1000$  using a near-infrared imager/spectrometer with a  $256 \times 256$  HgCdTe (NICMOS3) array. Generally, a set of at least two spectra were taken with the object dithered to two different positions along the slit. The spectrum of the comparison star HR 2714 (A2 V spectral type), after removing the hydrogen lines in its spectrum, was used to ratio the spectra of V838 Mon. HR 2714 is spatially close to V838 Mon ( $\sim 3^\circ$  away), and furthermore its spectra were recorded immediately preceding or after the V838 Mon observations. Thereby it is ensured that the object and the comparison star are observed at similar air mass. The ratioing process should therefore reliably remove telluric lines in the V838 Mon spectra. Wavelength calibration was accomplished using OH sky lines that register with the spectra. Spectral reduction and analysis were performed using IRAF. The observational details are presented in Table 1.

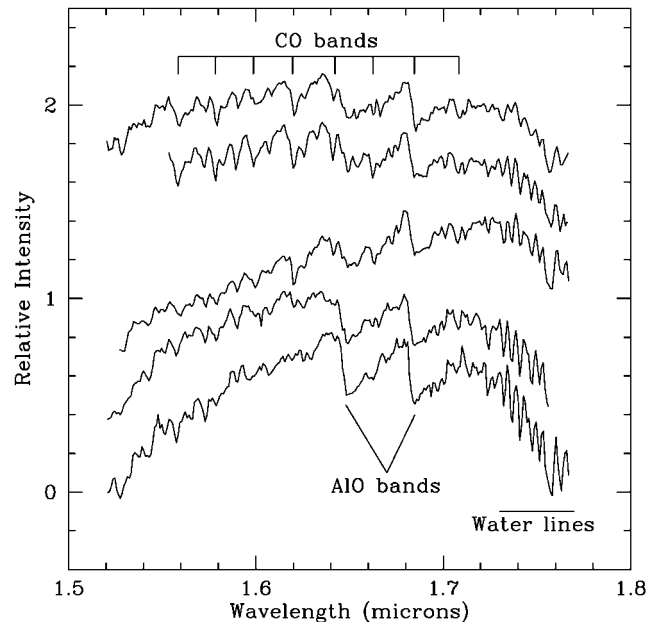


FIG. 1.—Near-IR *H*-band spectra of V838 Mon. *Bottom to top*: For 2002 November 20, 2003 January 25, 2003 December 14, 2004 April 15, and 2004 Dec 25. The prominent water lines are marked. Also shown are the positions of the second-overtone ( $\Delta\nu = 3$ ) band heads of  $^{12}\text{CO}$ . The prominent (1, 0) AIO molecular bands arising from the  $A^2\Pi_r-X^2\Sigma^+$  band system can be seen. The spectra have been offset by arbitrary amounts in intensity units for clarity of presentation. However, the true continuum strength at the *H*-band center ( $1.65 \mu\text{m}$ ) can be estimated from broadband photometric fluxes available on days close to our observations (Crause et al. 2005). For the spectra from bottom to top, these are  $H = 5.31, 5.53, 5.87, 5.92,$  and  $6.18$  mag, respectively.

## 3. RESULTS

The *H*-band spectra are shown in Figure 1. Apart from several prominent absorption features beyond  $1.73 \mu\text{m}$ , which we establish below to be due to water, there are other strong features in the spectra attributable to AIO and the second overtone of  $^{12}\text{CO}$ . We briefly discuss these features here, but a more comprehensive modeling and analysis of their evolution, supplemented by our simultaneous *J*- and *K*-band spectra in which these molecules have strong spectral signatures, will be presented in a future work. This work will also incorporate our *JHK* photometry results between 2002 and 2004. The most prominent features in Figure 1 are the deep absorption features at  $1.6480$  and  $1.6837 \mu\text{m}$ , which are due to the (1, 0) vibronic transitions from the *A*-*X* band system of the AIO radical. Along with its possible analog V4332 Sgr, V838 Mon appears to be the only other object to show these rare AIO bands (Banerjee et al. 2003). AIO also has a strong (4, 0) *A*-*X* band in the *J* band, which can be seen in the spectra of Lynch et al. (2004) and Evans et al. (2003). The expected positions of the  $^{12}\text{CO}$  first-overtone bands ( $\Delta\nu = 3$ ) are marked in Figure 1. Transitions from 3–0 to 7–4 are fairly prominent, especially in the later spectra. In general, the CO emission in V838 Mon is rather complex, especially in the first-overtone bands starting from  $2.29 \mu\text{m}$  in the *K* band. These first-overtone CO overtone bands are unusually deep in V838 Mon and show a very complex structure and evolution (Banerjee & Ashok 2002; Lynch et al. 2004; Evans et al. 2003). Integrated modeling, using both *H*- and *K*-band spectra, is necessary in order to understand the behavior of CO in V838 Mon.

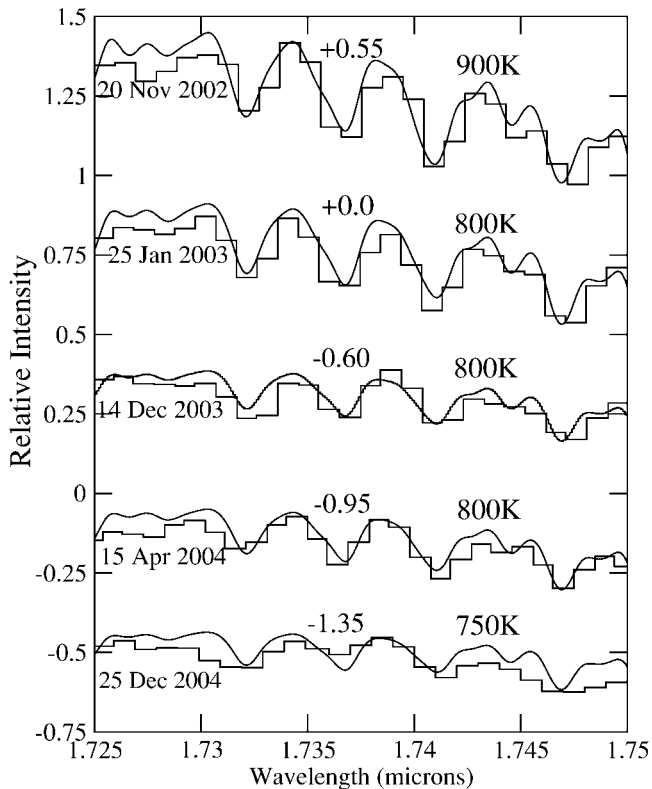


FIG. 2.—Synthetic spectra (solid curves) superposed on the observed data (in binned form) for the different epochs of observation. The observed spectra were normalized to unity at  $1.65 \mu\text{m}$  and for clarity are offset by the additive constants indicated above each spectrum.

### 3.1. Synthetic Spectra of Water

Our focus in this study is on the presence of water in V838 Mon. We tested for the signature of water in the spectra using the BT2 line list (R. J. Barber et al. 2005, in preparation). BT2 is a variational line list, computed at University College London using the DVR3D suite of programs, which calculates the rotation-vibration spectra of triatomic molecules (Tennyson

et al. 2004). It is the most complete water line list in existence, comprising over 500 million transitions (65% more than any other list), and is also the most accurate (over 90% of all known experimental energy levels are within  $0.3 \text{ cm}^{-1}$  of the BT2 values). The final module of the DVR3D suite, “SPECTRA,” was used to generate synthetic spectra at the appropriate wavelengths and temperatures, the output being convolved at  $4 \text{ cm}^{-1}$  (similar to the resolving power of the instrument). Finally, the output was “binned” with the same bin sizes and positions as the observed spectrum. Water features were clearly identified. Moreover, the relative intensities of the various features in the synthetic spectra are temperature dependent, and by testing for a best fit with the observed spectra, it was possible to determine the temperature of the region within which absorption was taking place on each of the five dates (Fig. 2). Figure 2 shows the best-fit temperature on each date. The observed spectra are shown as histograms, while the synthetic spectra are presented in their unbinned form. It can be seen from Figure 2 that between 2002 November 20 and 2004 December 5, the temperature at which absorption occurred decreased from  $900 \pm 30$  to  $750 \pm 50 \text{ K}$ , that is to say, a reduction of  $150 \pm 60 \text{ K}$  over a period of 767 days.

Many of the transitions within the BT2 line list have been labeled, and consequently it was possible to assign the 17 strong lines comprised by the five main absorption features in Figure 2. The details are given in Table 2. The lower and upper levels for each of these transitions are labeled in the manner  $(\nu_1\nu_2\nu_3)[JK_AK_C]$ , where the terms in parentheses are the vibrational quantum numbers and those in brackets represent the asymmetric top rotational quantum number and its projection onto two orthogonal axes (A and C), respectively. It can be seen that with the exception of one line at  $1.74454 \mu\text{m}$ , all of these strong transitions are in the (000)–(011) band. Table 2 also contains information about intensity. The second column gives the relative intensities of the 17 strongest synthetic  $\text{H}_2\text{O}$  lines in the wavelength range  $1.726\text{--}1.751 \mu\text{m}$  at a temperature of 800 K, while the last column gives the relative intensity of the five strong absorption features that are the result of the blending of these lines. The intensity is expressed as the total integrated line intensity within the bin whose position corre-

TABLE 2  
LINE CENTER AND RELATIVE INTENSITY DETAILS

$\lambda$ ( $\mu\text{m}$ )	$I(\text{line})^a$ Rel.	Lower Level $(\nu_1\nu_2\nu_3)[JK_AK_C]$	Upper Level $(\nu_1\nu_2\nu_3)[JK_AK_C]$	Center ( $\mu\text{m}$ )	$I(\text{feat.})^b$ Rel.
1.73202 .....	1.93	(0 0 0)[7 3 4]	(0 1 1)[8 5 3]	1.7329	1.77
1.73239 .....	1.61	(0 0 0)[6 3 4]	(0 1 1)[7 5 3]		
1.73686 .....	2.83	(0 0 0)[9 2 7]	(0 1 1)[10 4 6]	1.73686	1.93
1.73987 .....	1.23	(0 0 0)[15 7 8]	(0 1 1)[16 7 9]		
1.74036 .....	2.07	(0 0 0)[15 5 10]	(0 1 1)[16 5 11]		
1.74082 .....	1.03	(0 0 0)[16 6 11]	(0 1 1)[17 6 12]	1.74071	2.21
1.74121 .....	1.91	(0 0 0)[15 6 9]	(0 1 1)[16 6 10]		
1.74128 .....	1.26	(0 0 0)[5 3 2]	(0 1 1)[6 5 1]		
1.74269 .....	1.27	(0 0 0)[14 8 7]	(0 1 1)[15 8 8]	Shoulder	1.36
1.74445 .....	1.24	(0 0 0)[7 0 7]	(0 1 1)[8 2 6]		
1.74454 .....	1.23	(0 0 0)[13 5 8]	(1 1 0)[14 6 9]	1.74456	1.77
1.74471 .....	1.12	(0 0 0)[13 9 4]	(0 1 1)[14 9 5]		
1.74650 .....	2.12	(0 0 0)[14 7 8]	(0 1 1)[15 7 9]		
1.74674 .....	2.29	(0 0 0)[6 2 5]	(0 1 1)[7 4 4]		
1.74680 .....	1.50	(0 0 0)[16 5 12]	(0 1 1)[17 5 13]	1.74688	2.59
1.74728 .....	1.36	(0 0 0)[8 2 6]	(0 1 1)[9 4 5]		
1.74750 .....	1.13	(0 0 0)[14 6 8]	(0 1 1)[15 6 9]		

<sup>a</sup> The relative intensities of the individual strong lines are computed at 800 K.

<sup>b</sup> The relative intensities of the features are computed for 2003 January 25.

sponds to that of maximum absorption within the feature. The apparent discrepancies between the two sets of data are explained by the fact that the features comprise not only the strong lines listed in Table 2, but a large number of weak lines, which, individually, are insignificant but collectively can make an important contribution to total absorption.

Lastly, it has been possible to estimate the H<sub>2</sub>O column densities using  $I = I_0 \exp(-\kappa_\lambda NS)$ , where  $N$  is the number of water molecules per centimeter,  $S$  is the distance in centimeters, and the product  $NS$  is the column density (molecules cm<sup>-1</sup>);  $\kappa_\lambda$  is the opacity at wavelength  $\lambda$  and is one of the outputs of SPECTRA. Once the best temperature fit had been established, the optimum values of  $I_0$  and  $NS$  that gave the best fit to the observed data were obtained. The effect of increasing  $I_0$  is to raise the overall level of the synthetic plot, while increasing  $NS$  has the effect of increasing the depth of the strong absorption features relative to the weak ones. The data used for this fitting, prior to applying the exponential factor above, were first convolved with a Gaussian with a FWHM of 1 cm<sup>-1</sup>, which is equivalent to a Doppler velocity spread of 50 km s<sup>-1</sup>. Such a velocity spread in the cool expanding shell around V838 Mon is suggested from the analysis by Lynch et al. (2004). Subsequently, the model data were convolved with a 4 cm<sup>-1</sup> FWHM Gaussian to take account of the resolving power of the instrument. Table 3 details our estimates of column density on each of the five dates. We believe that our methodology is liable to suffer from systematic errors, and consequently we estimate the errors as being  $^{+100}_{-50}$ %. However, the comparison between the column densities at the different dates will be more accurate, and we estimate the error in the relative numbers at  $^{+25}_{-20}$ %.

#### 4. DISCUSSION

We have compared our column density and temperature estimates with those derived by Lynch et al. (2004). The temperature of  $800 \pm 30$  K on 2003 January 25 is consistent with

TABLE 3  
TEMPERATURE AND COLUMN DENSITIES

Observation Date	Temperature (K)	Error (K)	Column Density (molecules cm <sup>-2</sup> )
2002 Nov 20 .....	900	30	$9.3 \times 10^{21}$
2003 Jan 25 .....	800	30	$9.0 \times 10^{21}$
2003 Dec 14 .....	800	30	$3.8 \times 10^{21}$
2004 Apr 15 .....	800	40	$5.1 \times 10^{21}$
2004 Dec 25 .....	750	50	$4.6 \times 10^{21}$

the 750–790 K suggested by Lynch et al. (2004) for the “cool cloud” surrounding V838 Mon based on observations of H<sub>2</sub>O and CO molecular bands and the SiO ( $2\nu$ ) feature made at about the same date. Our estimate of the H<sub>2</sub>O column density on 2003 January 25 is ~63% of the Lynch et al. value at a similar date and is therefore in reasonably good agreement (within our estimated error) with their work. The presence of an envelope at ~800 K around V838 Mon, as our analysis shows, confirms the findings of Lynch et al. that a cool cloud surrounds the central star of V838 Mon. The derived temperature of 800 K is close to that expected for an expanding graybody that absorbs stellar energy in the visible/near-IR and reradiates it at longer wavelengths (see eq. [4] of Lynch et al. 2004). If the cooling of the water-bearing envelope continues at the suggested rate of ~75 K per year, its temperature may reach the ice sublimation temperature (~150 K) to form water ice in a few years from now. Such a development would further enhance the similarity between V838 Mon and its possible analog V4332 Sgr, in which water ice is detected strongly 10 years after the object’s outburst (Banerjee et al. 2004).

Research work at the Physical Research Laboratory is funded by the Department of Space, Government of India. R. J. B. wishes to thank the Particle Physics and Astronomy Research Council for its financial support. We also thank the anonymous referee for helpful comments.

#### REFERENCES

- Banerjee, D. P. K., & Ashok, N. M. 2002, *A&A*, 395, 161  
 ———. 2004, *ApJ*, 604, L57  
 Banerjee, D. P. K., Varricatt, W. P., & Ashok, N. M. 2004, *ApJ*, 615, L53  
 Banerjee, D. P. K., Varricatt, W. P., Ashok, N. M., & Launila, O. 2003, *ApJ*, 598, L31  
 Bond, H. E., et al. 2003, *Nature*, 422, 405  
 Brown, N. J. 2002, *IAU Circ.* 7785  
 Carr, J. S., Tokunaga, A. T., & Najita, J. 2004, *ApJ*, 603, 213  
 Crause, L. A., Lawson, W. A., Menzies, J. W., & Marang, F. 2005, *MNRAS*, 358, 1352  
 Crause, L. A., Lawson, W. A., Warrick, A., Kilkenny, D., van Wyk, F., Marang, F., & Jones, A. F. 2003, *MNRAS*, 341, 785  
 Crovisier, J., Leech, K., Bockelée-Morvan, D., Brooke, T. Y., Hanner, M. S., Altieri, B., Keller, H. U., & Lellouch, E. 1997, *Science*, 275, 1904  
 Dello Russo, N., Bonev, B. P., DiSanti, M. A., Mumma, M. J., Gibb, E. L., Magee-Sauer, K., Barber, R. J., & Tennyson, J. 2005, *ApJ*, 621, 537  
 Desidera, S., et al. 2004, *A&A*, 414, 591  
 Evans, A., Geballe, T. R., Rushton, M. T., Smalley, B., van Loon, J. T., Eyres, S. P. S., & Tyne, V. H. 2003, *MNRAS*, 343, 1054  
 Geballe, T. R., et al. 2002, *ApJ*, 564, 466  
 Henden, A., Munari, U., & Schwartz, M. 2002, *IAU Circ.* 7859  
 Hinkle, K. H., & Barnes, T. G. 1979, *ApJ*, 227, 923  
 Jennings, D. E., & Sada, P. V. 1998, *Science*, 279, 844  
 Kaminsky, B. M., & Pavlenko, Ya. V. 2005, *MNRAS*, 357, 38  
 Kimeswenger, S., Lederle, C., Schmeja, S., & Armsdorfer, B. 2002, *MNRAS*, 336, L43  
 Kipper, T., et al. 2004, *A&A*, 416, 1107  
 Lançon, A., & Rocca-Volmerange, B. 1992, *A&AS*, 96, 593  
 Lane, B. F., Retter, A., Thompson, R. R., & Eisner, J. A. 2005, *ApJ*, 622, L137  
 Lynch, D. K., et al. 2004, *ApJ*, 607, 460  
 Munari, U., et al. 2002, *A&A*, 389, L51  
 ———. 2005, *A&A*, 434, 1107  
 Neufeld, D. A., Feuchtgruber, H., Harwit, M., & Melnick, G. J. 1999, *ApJ*, 517, L147  
 Polyansky, O. L., Zobov, N. F., Viti, S., Tennyson, J., Bernath, P. F., & Wallace, L. 1997, *ApJ*, 489, L205  
 Retter, A., & Marom, A. 2003, *MNRAS*, 345, L25  
 Ryde, N., Lambert, D. L., Richter, M. J., & Lacy, J. H. 2002, *ApJ*, 580, 447  
 Soker, N., & Tylenda, R. 2003, *ApJ*, 582, L105  
 Spinrad, H., & Newburn, R. L., Jr. 1965, *ApJ*, 141, 965  
 Tennyson, J., Kostin, M. A., Barletta, P., Harris, G. J., Polyansky, O. L., Ramanlal, J., & Zobov, N. F. 2004, *Comput. Phys. Commun.*, 163, 85  
 Tsuji, T. 2001, *A&A*, 376, L1  
 Tylenda, R. 2004, *A&A*, 414, 223  
 Tylenda, R., Soker, N., & Szczerba, R. 2004, *A&A*, submitted (astro-ph/0412183)  
 van Loon, J. T., Evans, A., Rushton, M. T., & Smalley, B. 2004, *A&A*, 427, 193  
 Wallace, L., Bernath, P., Livingston, W., Hinkle, K., Busler, J., Guo, B., & Zhang, K. 1995, *Science*, 268, 1155  
 Wisniewski, J. P., Bjorkman, K. S., & Magalhães, A. M. 2003a, *ApJ*, 598, L43  
 Wisniewski, J. P., Morrison, N. D., Bjorkman, Miroshnichenko, A. S., Gault, A. C., Hoffman, J. L., Meade, M. R., & Nett, J. M. 2003b, *ApJ*, 588, 486